The Seismic Sequences of December 2015 (M_L= 4.3) and May 2016 (M_L = 4.9) in Guadalajara, Jalisco, México

Francisco Javier Núñez Cornú[1], Walter Manuel Rengifo[1], Felipe de Jesús Escalona Alcázar [2] , Diana Núñez[1], Claudia Beatriz Quinteros Cartaya[1], Elizabeth Trejo Gómez[1], Carlos Suárez Plascencia[1]

[1] C. A. Centro de Sismología y Volcanología de Occidente (SisVOc). Universidad de Guadalajara, Centro Universitario de la Costa, Avenida Universidad 203, Puerto Vallarta, Jal. México

[2]Unidad Académica Ciencias de la Tierra, Universidad Autónoma de Zacatecas, Calzada de la Universidad 108, Zacatecas, Zac., MÉXICO, CP 98080

Corresponding Author:

Francisco Javier Núñez Cornú, pacornu77@gmail.com, Tel. 51 322 226 2229
Centro de Sismología y Volcanología de Occidente, Universidad de Guadalajara

Keywords: Crustal seismicity; Seismic hazard; Jalisco Block; Guadalajara, Jal.; Zapopan Graben

Abstract

Historically, the city of Guadalajara has been affected not only by great regional earthquakes (M > 7.0) associated with the subduction process and regional crustal structures but also by local seismic sequences, that caused moderate to severe structural damage to buildings, whose source is not clear. Between December 2015 and May 2016, two seismic sequences occurred, affecting the city of Guadalajara. Both seismic sequences were recorded by the Jalisco Seismic Accelerometric Telemetric Network. The preliminary locations for May 2016 sequence estimated by the Antelope automatic system show alignment with an NNE-

SSW trend, west of the city of Guadalajara. The subsequent relocations of theses earthquakes show two N-S alignments at the west of the city of Guadalajara, which agree with December 2015 hypocenters. The focal mechanisms analysis of the earthquakes shows that most of them correspond to normal fault mechanisms that are parallel to the hypocentral alignments suggesting the existence of two active faults responsible for the seismic sequences. Furthermore, these structures might constitute a graben, which we refer to as Zapopan Graben. Additionally, we calculated that these faults are 21 and 28 km length, respectively, which indicates that could have the potential to generate shallow earthquakes that reach magnitudes of 6.2 and 6.5, and could cause significant damages in the Guadalajara Metropolitan Zone.

Introduction

The Guadalajara Metropolitan Zone (GMZ) includes the towns of Guadalajara, Zapopan, Tlaquepaque, Tonalá, and Tlajomulco is located near the intersection of the Tepic-Zacoalco Rift (TZR), the Colima Rift (CR) and the Chapala - Tula Rift (CTR) (Fig. 1).

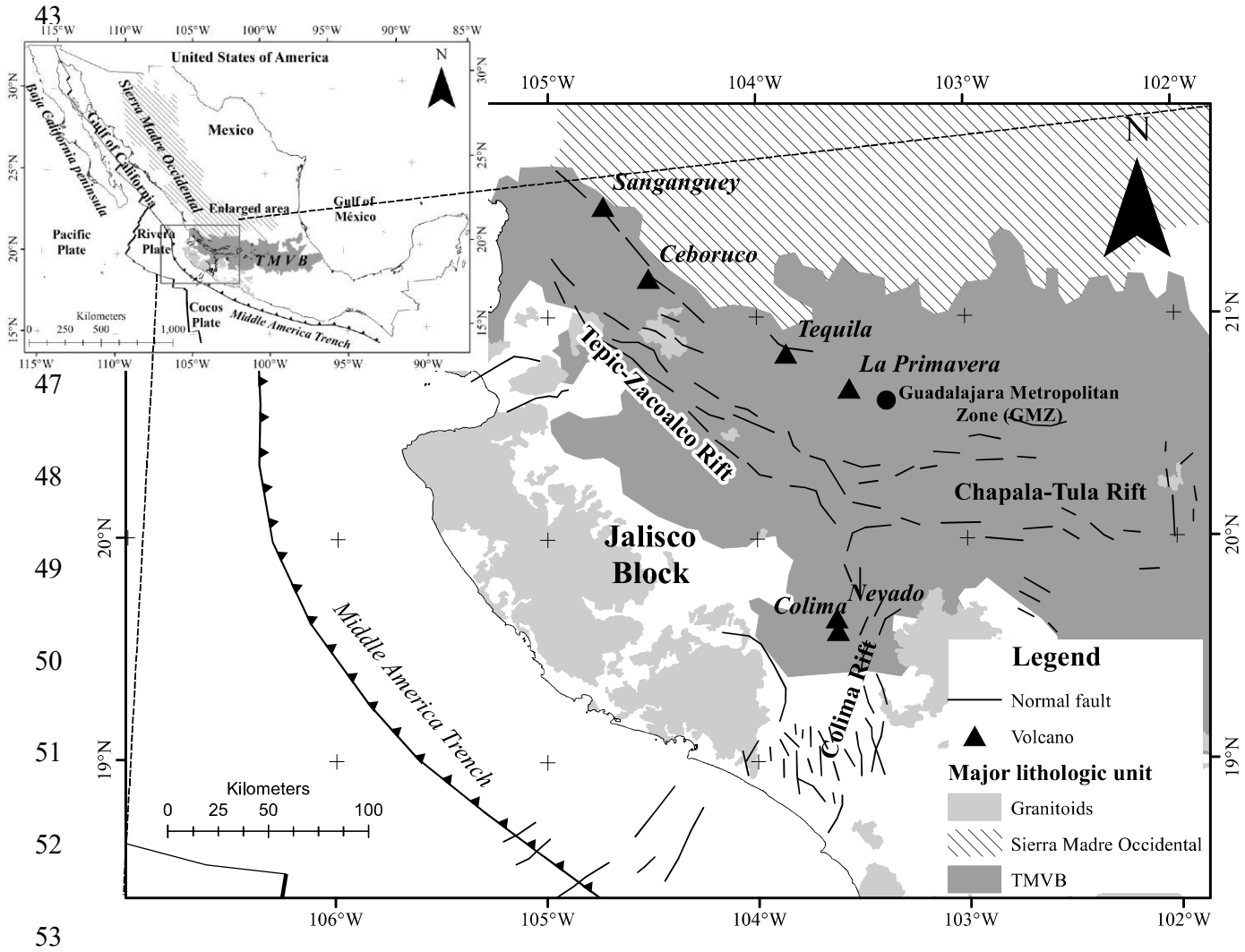

Figure 1. Tectonic setting of the region. TMVB: TransMexican Volcanic Belt.

The GMZ and its surroundings rest on two great volcano-sedimentary plains, the Atemajac, and Tesistán (Fig. 2). In this area, the population in 1912 was 210,839 inhabitants (Dirección General de Estadística, 1910). By 1950, it reached 902,987 inhabitants. In 1957, the GMZ began to take shape with the construction of the Industrial Zone in the south of Guadalajara. This fact was a turning point in the urban progression of the city, catapulting the expansion of the urban layout and its population growth. By 1964, the population reached one million inhabitants and an approximate area of 90 km^2, with a density of 11,111 people/km^2 and by 2015, it reached 4.5 million people, an area of approximately 2,900 km^2 and a density of 1,552 people/km^2, representing about 60% of the total population of the Jalisco state. The accelerating increase of the urban layout has been sustained by the development of industry, commercial activities and services, which projects the city in the long term as an essential role of demographic attraction, urbanizing surrounding agricultural lands over the entire northwest sector on the plain of Tesistán (Fig. 2).

Currently, GMZ is the second most populated city in Mexico. In this scenario, the La Primavera Caldera is located in the western part of GMZ, within the Zapopan Municipality, and a geothermal project is being developed in this area by the Federal Electricity Commission.

The GMZ has a high seismic hazard according to historical reports of both large and medium earthquakes, and local seismic swarms (Waitz and Urbina, 1919; Arreola-Ochoa, 2015). For this reason, it is essential to evaluate and identify the seismogenic structures that exist in the area to assess the seismic hazard that these structures can present both to the population of the GMZ and the infrastructure, including the facilities of the Geothermal Plant at Cerritos Colorados inside the La Primavera Caldera.

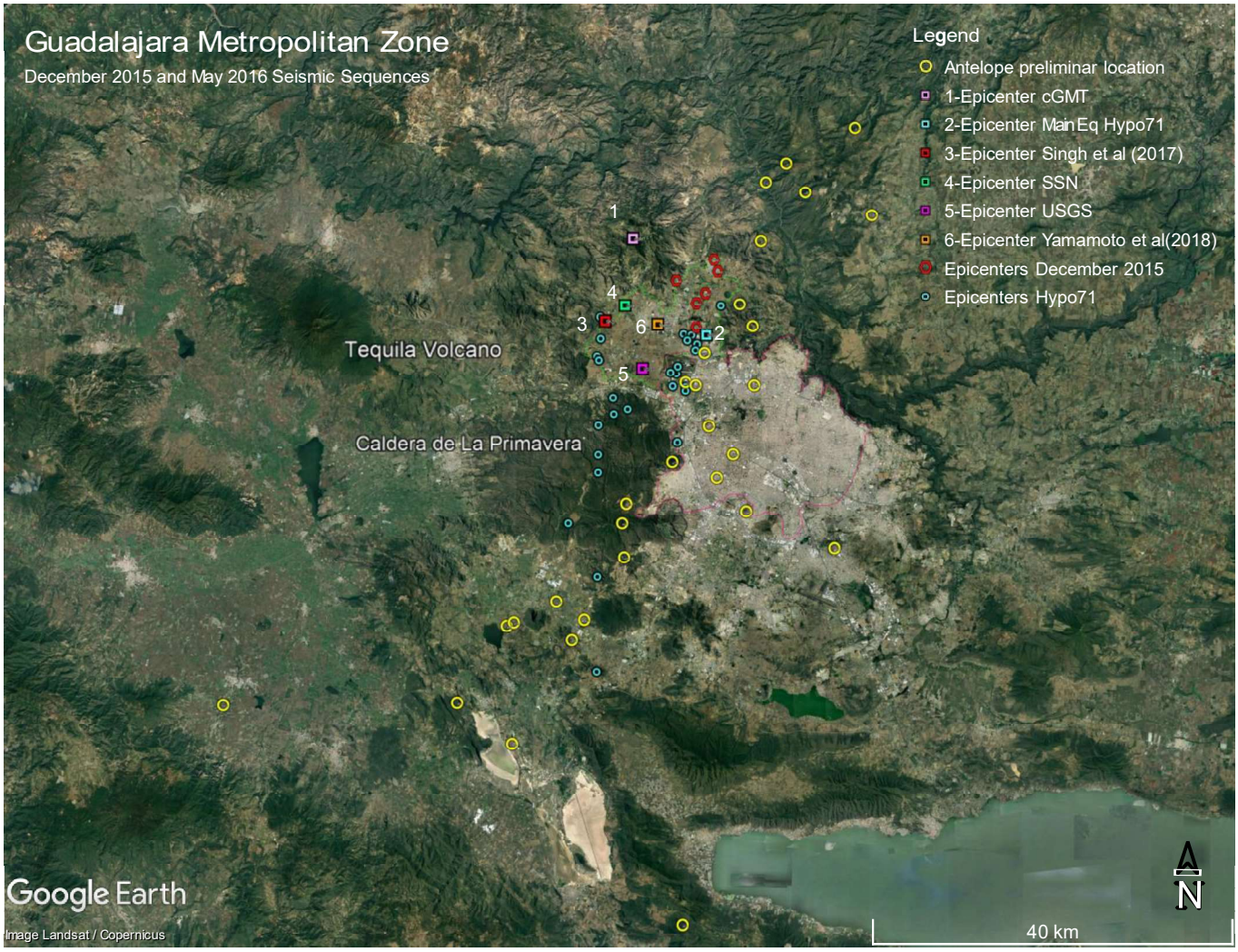

89 Figure 2. Preliminary Antelope locations and Hypo71 relocations for December 2015 and May 2016
90 seismic swarms. Different epicentral locations reported from different sources for May 2016 Main
91 Earthquake. Tesistán (red line) and Atemajac (green line) structures limits shown over the
92 Guadalajara Metropolitan Zone (GMZ) (Map data: Google Earth: Image @2020 CNES/Airbus,
93 @2020 Maxar Technologies).

94

95 In December 2015, a seismic sequence began with an M_L= 4.2 earthquake; this seismic
96 sequence was studied by Marín-Mesa *et al.* (2019). The second sequence began on May 11,
97 2016, with an earthquake M_L = 4.9 that took place at the GMZ. Different locations for the
98 hypocenter were reported by different agencies: the hypocenter reported by USGS is

20.751ºN, 103º.499ºW, depth 10 km, mb = 4.5. gCMT reports 20.88°N, 103.51°W, depth:17.4 km, Mw = 4.9; Normal Fault, Fault plane: strike 23°, dip=46°, slip-87°. The Servicio Sismológico Nacional (SSN) reports 20.8135ºN, 103.518ºW depth = 8 km, M = 4.8 (Fig.2). Here, we analyze the data for this earthquake and its aftershocks registered by a local seismic network.

Tectonic Setting

The study area is located on the Jalisco Block (JB) in western Mexico (Fig. 1). It is close to the intersection between the Late Oligocene-Early Miocene Sierra Madre Occidental (SMO) silicic province and the Late Miocene to recent Trans Mexican Volcanic Belt (TMVB) basaltic to andesitic arc magmatism (Fig. 1). The tectonic boundary of the Jalisco Block to the North is the TZR (Bandy *et al.,* 1995; Ferrari and Rosas-Elguera, 1999). The TZR formed at the end of the Miocene, and it is oriented NW-SE with a length of 250 km and a maximum width of 50 km (Frey *et al.*, 2007). The eastern boundary is an N-S structure of 190 km length and 30 to 60 km width, known as the CR (Allan, 1986). Towards the south, the boundary is the Middle American Trench (MAT) along which the Rivera and Cocos plates are subducted beneath the North American plate.

The detachment of the JB from North American plate began in the Early Pliocene (Luhr *et al.*, 1985) and is a response to the rifting of the Gulf of California and subsequent extension (Luhr *et al.*, 1985; Allan *et al.*, 1991). The movement along the TZR and CTR has been considered to be either NW-SE (Luhr *et al.*, 1985; Allan, 1986; Bourgois and Michaud, 1991) or SW-NE (Ferrari *et al.*, 1994; Selvans et al., 2011). DeMets and Stein (1990) and Rosas-

121 Elguera et al. (1996) support that the movement of the JB to the NW could be due to the
122 oblique subduction of the Rivera and Cocos plates respect to North America (Núñez-Cornú
123 *et al.*, 2002), combined with plate rearrangement due to the separation of the Baja California
124 peninsula from mainland Mexico (Luhr *et al.*, 1985). The subduction velocity varies from
125 1.2 to 2.3 cm/year according to distance to the pole (Minster and Jordan, 1978). Deformation
126 within the JB is extensional (Kostoglodov and Bandy, 1995) though maybe insignificant
127 (Duque-Trujillo *et al.*, 2014).

128 Along the northern JB boundary, in the TZR region, the deformation started at the end of the
129 Miocene and continues to present. During this time, the volcanism varies from subduction-
130 related to intraplate (Righter and Carmichael, 1992; Rosas-Elguera *et al.,* 1996). The major
131 stratovolcanoes such as Sangangüey, Ceboruco, Tequila, among others, formed during the
132 initial stages of the TMVB formation (Ferrari and Rosas-Elguera, 1999). At the edge of the
133 TZR, the faults constituted during the Pliocene acted as channels to the magma migration
134 and favored the formation of monogenetic volcanoes; most of them align with the major NW-
135 SE and N-S faults, suggesting a structural control (Ferrari and Rosas-Elguera, 1999; Rossotti
136 *et al*., 2002). Within the TZR, the La Primavera Caldera is at the end of a long-lived silicic
137 upper crustal chamber that is at the cooling stage; however, it has enough heat to develop a
138 geothermal system (Maciel-Flores and Rosas-Elguera, 1992).

139

140 **Historical Seismicity**

141 The Jalisco region has experienced numerous destructive earthquakes of great magnitude
142 with epicenters along the coast and inland. The historical macroseismic data for the region

143 date back to 1544 (Núñez-Cornú, 2011), with at least 22 major earthquakes with M ≥ 7.0
144 reported in the past 474 years (Núñez-Cornú *et al.,* 2018) (Fig. 3). Recently, Suter (2018,
145 2019a, 2019b, 2020a, and 2020b) has studied and reviewed some of the historical
146 earthquakes in Jalisco that have caused significant damage. Suter (2019a) studied and
147 concluded that 1563, May 27, M_I = 8.0, earthquake took place offshore Puerto de Navidad
148 (now named as Barra de Navidad), and the estimated rupture area can be compared to the
149 1932 and 1995 earthquakes. The 1567 Ameca, Jalisco Earthquake, December 28, Mw = 7.2,
150 was also studied by Suter (2015, 2019a, 2020b). The earthquake doublet of October 22-23,
151 1749 at the northern Colima Graben (1749a and 1749b, Fig. 3) was revised by Suter (2019b).
152 The November 6, 1774, M_I = 6.0 Bolaños Graben Earthquake (Fig 3) is described by Suter
153 (2020a).

154 Suter (2018) analyzed the macroseismic data of October 2, 1847, Jalisco Earthquake, and
155 concluded that there were two earthquakes the same day. The first one, a subduction type
156 earthquake, took place at 07:30 am offshore Tecomán, Colima with an estimated magnitude
157 of Mw = 7.4 (1847a-Fig. 3). The second one, a shallow intraplate type earthquake with an
158 estimated magnitude M_I = 5.7 (1847b-Fig. 3), took place at 09:30 am and affected the western
159 part of the CTR, destroying the city of Ocotlán and other towns nearby. Last century six big
160 earthquakes took place: 1932, June 03 M = 8.2; 1932, June 18, M = 7.8; 1934, November
161 30, M = 7.2; 1941, April 15, M = 7.9; 1948, December 3, M = 7.0; 1995, October 9. At date,
162 27 big destructive earthquakes occurred in Jalisco have been identified (Fig. 3), and most of
163 them have been associated with the subduction process and/or active crustal faults. There
164 also occurred earthquakes with magnitude greater than 6.0 and less than 7.0 in the region.

For the period 1918 to 1973, Singh *et al*. (1984) reported 17 earthquakes; while for the period 1973 – 2020, the SSN reports ten earthquakes in this region.

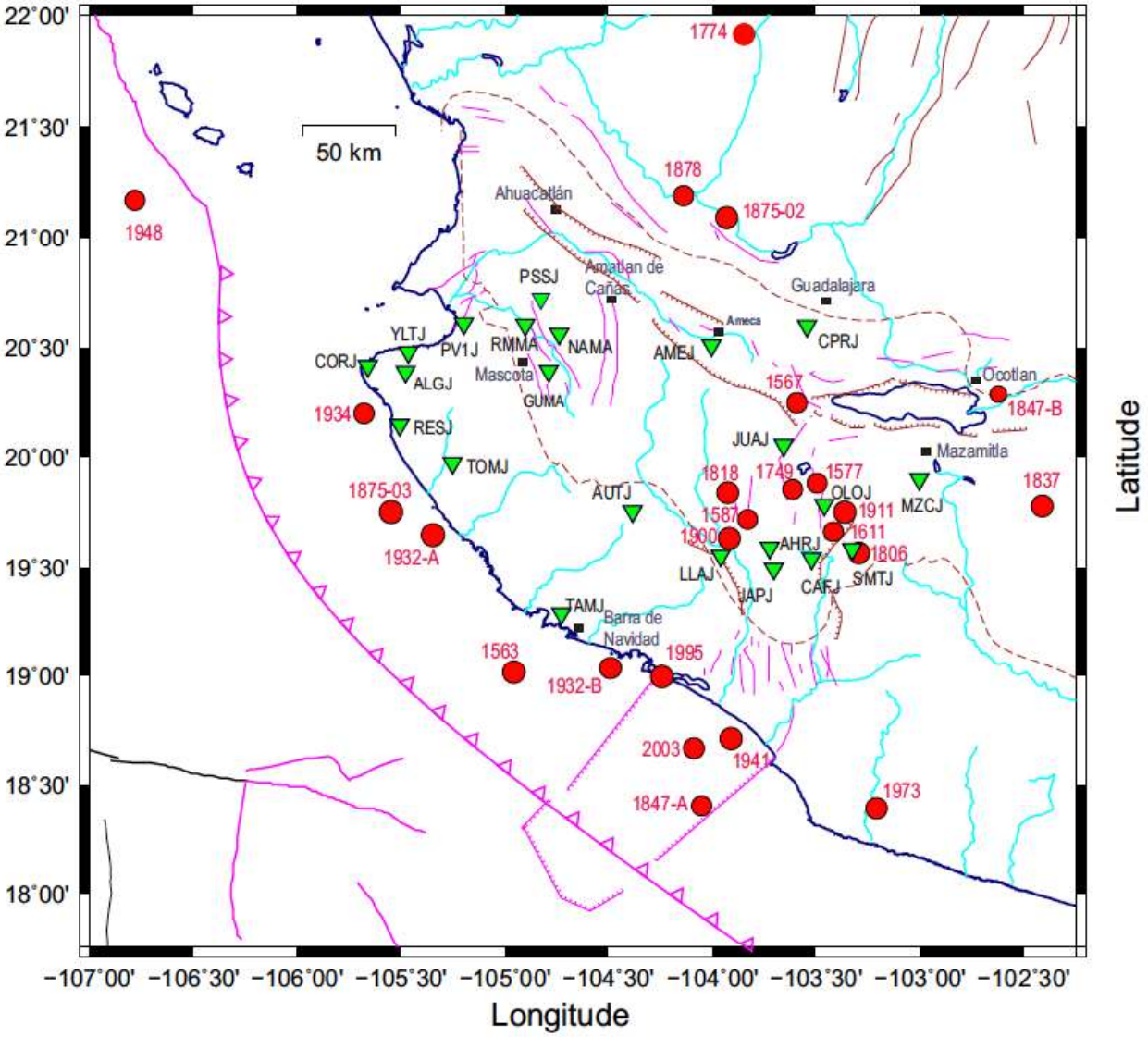

Figure 3. Seismic stations (inverted green triangles) that recorded the May 11-13, 2016 seismic sequence. Historical destructive earthquakes (red circles) near or within the Jalisco Block after Núñez-Cornú *et al*. (2018) and Suter (2015, 2018, 2019a, 2019b, 2020a, 2020b).

Moreover, destructive seismic swarms that occurred in the inland region of Jalisco have also been reported. The first record of seismic swarms in the GMZ was reported by the Commission on the earthquakes of February 1875 (Matute, 1875), who referred to the events between 1685 and 1687. The seismic sequence of 1749 - 1750 was reported by Martínez Gracida, (1886), and Orozco y Berra, (1887). Waitz and Urbina (1919) list the occurrence of other series of events at GMZ in the following periods: between 1770 and 1771 reported by Martínez-Gracida (1886) and Orozco and Berra (1887); in 1783 in the zone of Ahuacatlán (Fig. 3), by Martínez-Gracida, (1886); in 1806 from March 25 to June at GMZ and in 1844 from March 27 to May 27, which alarmed the population of Guadalajara and its surroundings. In 1912 from May 8 to September 10 (Ordoñez, 1912), a seismic swarm affected the municipalities of Guadalajara and Zapopan, alarming the population. Arreola-Ochoa (2015) described this episode "Because of the earthquakes, many families fled the city." Headlines of the newspapers give us an idea of the environment that was serious for those days in the city: "Three-quarters of its inhabitants migrate from Guadalajara, Guadalajara continues to shake." Waitz and Urbina (1919) reported that in May of 1912, 54 events occurred, classifying them into seven strong, ten somewhat strong and 37 light and very light. In the first week of June of that year, 11 events were reported, two somewhat strong and nine very light to light. The tectonic stresses in the area are complex since the three rifts (TZR, CR, CTR) converge; however, it is not known which is the possible seismic source of these seismic sequences. In March 1989, an earthquake swarm took place in the zone of Ameca – Amatlán de Cañas (Fig. 3) (Núñez-Cornú *et al.*, 2002). Two seismic sequences occurred from December 15, 2015, until December 20 and during May 11 and May 13, 2016, but only the

mainshocks were felt like a jolt. The instrumental near field data of this seismicity are the first to be available for the GMZ region.

Data and Methods

The Jalisco Seismic Accelerometric Telemetric Network (RESAJ) was designed to research and analyze the potential for destructive earthquakes within the Jalisco region (Núñez- Cornú *et al.,* 2018). Each RESAJ station has a 24 bit A/D Quanterra Q330 6Ch or Q330S 6ch DAS digitizer, a Lennartz LE 3D (1 Hz) seismometer, and a Kinemetrics triaxial accelerometer model FBA ES-T. Data are transmitted in real-time to the Central Lab at Centro de Sismología y Volcanología de Occidente (SisVOc) in Puerto Vallarta. Data acquisition was carried out using the Antelope system (Lindquist *et al*., 2007).

The first sequence took place between December 5 – 20, was studied by Marín-Mesa *et al*. (2019), who reported seven earthquakes located in the GMZ, at North of the city of Zapopan, with an NNE-SSW alignment direction along 7.8 km, depths < 20 km, and M_L < 3.0. The composite focal mechanism calculated from three earthquakes indicated normal fault on a plane in agreement with the epicentral alignment.

The second seismic sequence began on May 11, 2016, at 22:35 GMT with an earthquake (M_L = 4.9), finishing by May 14 at 23:00 GMT. For this seismic sequence, 17 RESAJ stations were operating and recording the data (Fig. 3); 3 more stations (RMMA, GUMA, NAMA) from a temporary seismic network, located at Mascota, Jalisco area, also recorded this activity. Five of the RESAJ stations are located less than 100 km from the epicentral zone. The Antelope system detected and located 40 earthquakes in the GMZ area, using the IASP91 velocity model, with magnitudes between 1.8 and 4.9. These preliminary locations of the

seismic sequence suggest an alignment NNE-SSW of the earthquakes across the western urban zone of GMZ (Fig. 2).

After reviewing the preliminary locations, the first step was to identify all the local earthquakes in the helicorders records at La Primavera Caldera station (CPRJ), the closest station to Guadalajara, to count the total number of events of the seismic sequence. The 11-14 May seismicity records were extracted from the Antelope database in mini seed format. This database was converted to a Seisan format (Haskov and Ottomeller, 1999) for the waveform analysis. The arrival times and polarities of the P waves were read from the vertical components, and S waves were read from the horizontal components; error in phase readings is less than 0.1 s. A total of 115 earthquakes were identified, from which we chose 54 events that were recorded by more than five RESAJ stations and had at least 5 P and 2 S wave arrival readings.

These earthquakes were relocated with the Hypo71 program (Lee and Lahr, 1972) using the velocity model (Fig. 4) proposed by Núñez-Cornú *et al.* (2002). Eight different depths were used as the initial solution to obtain the best solution. Those with the lowest location errors were selected. The media error values solutions obtained were: Root Mean Square (RMS): 0.49s; the standard error of the epicenter (ERH): 3.7 km; and the standard error of the focal depth (ERZ): 2.0 Km. (Table 1). The local magnitude relation (Lay and Wallace, 1995) was used in this study.

250

Num	Yr	mo	day	ho	min	sec	Lat	Long	Depth (Km)	Mag	RMS	ERH	ERZ	Gap	Dist	NL
w0	16	5	11	22	35	18.8	20.78483	-103.43130	9.85	4.92	0.51	2.3	1.6	247	24.1	29
w1	16	5	11	22	45	8.65	20.74600	-103.46320	10.58	2.50	0.23	2.6	2.2	243	18.7	8
w2	16	5	11	22	47	25.6	20.75300	-103.46170	11.66	3.13	0.44	2.6	1.8	244	19.5	19
w3*	16	5	11	22	50	2.84	20.72133	-103.53020	7.55	2.70	0.61	5.7	6.9	238	14.0	10
w5*	16	5	11	23	15	53.3	20.70517	-103.52930	7.92	2.58	0.57	8.8	13.5	237	77.6	8
w6	16	5	11	23	22	43.5	20.75883	-103.54550	14.35	1.83	0.35	3.7	1.4	240	18.1	11
w7	16	5	11	23	45	9.48	20.67783	-103.46170	13.55	3.16	0.72	3.3	1.7	238	12.5	26
w8	16	5	11	23	56	23.8	20.78550	-103.45570	9.69	2.57	0.43	4.3	4.9	246	23.0	9
w10*	16	5	12	0	34	21.2	20.71017	-103.51470	18.47	2.27	0.67	5.7	2.0	238	13.1	11
w12	16	5	12	1	18	47.6	20.73250	-103.45330	12.64	3.03	0.55	2.5	1.6	243	17.9	25
w13	16	5	12	1	29	33.9	20.77550	-103.44130	5.00	2.95	0.49	2.3	3.5	246	22.6	21
w14	16	5	12	2	1	41.4	20.76267	-103.54750	16.62	2.53	0.23	3.4	1.1	320	18.6	8
w15	16	5	12	2	30	59.2	20.78017	-103.54380	17.01	2.43	0.19	3.7	1.3	321	20.5	7
w16*	16	5	12	3	21	36.2	20.64733	-103.54550	12.98	2.64	0.61	4.4	1.9	232	5.8	14
w17	16	5	12	4	28	29.7	20.73333	-103.46700	11.36	2.50	0.40	2.3	1.7	242	17.3	19
w19	16	5	12	4	49	49	20.78450	-103.44730	9.05	2.49	0.34	2.0	1.8	247	88.0	16
w20*	16	5	12	5	30	14.7	20.54383	-103.54550	11.78	2.17	0.50	4.6	4.3	139	5.7	19
w21*	16	5	12	5	32	37.3	20.66483	-103.54550	21.80	2.06	0.81	6.2	5.3	257	7.7	11
w24	16	5	12	8	29	25.3	20.76933	-103.44300	8.66	2.34	0.47	2.6	2.6	249	22.0	19
w26	16	5	12	10	50	25.7	20.81383	-103.41620	12.64	2.51	0.30	3.0	1.6	250	27.6	11
w28*	16	5	12	14	8	42.1	20.69383	-103.54550	14.75	2.11	0.67	5.4	2.9	235	10.9	9
w29*	16	5	12	15	26	27.9	20.59683	-103.57670	10.61	1.50	0.66	7.1	5.3	177	3.4	8
w31	16	5	12	18	22	8.53	20.74700	-103.46930	12.37	2.03	0.31	3.8	3.4	243	18.5	9
w32	16	5	12	18	24	7.21	20.80200	-103.54450	19.85	2.16	0.03	1.1	0.7	322	22.9	8
w33	16	5	13	15	17	9.59	20.45017	-103.54550	15.00	2.25	0.60	5.9	9.2	136	16.1	11
w35	16	5	13	19	7	32.3	20.72883	-103.45330	11.04	2.55	0.74	3.7	3.0	242	62.6	22
w36	16	5	13	10	37	59.1	20.77917	-103.45170	7.59	2.55	0.40	1.8	2.0	246	22.5	26

251

252 Table 1. Earthquakes relocated for the May 2016 seismic swarm. *Mag*: Local mag; *RMS*: Root mean
253 square error of time residuals in sec; *ERH*: Standard error of the epicenter in km; *ERZ*: Standard error
254 of the focal depth in km; *Gap*: Largest azimuthal separation in degrees between stations; *Dist*:
255 Epicentral distance in km to the nearest station; *NL*: number of phase readings. * Epicenters inside
256 La Primavera Caldera.

257

258

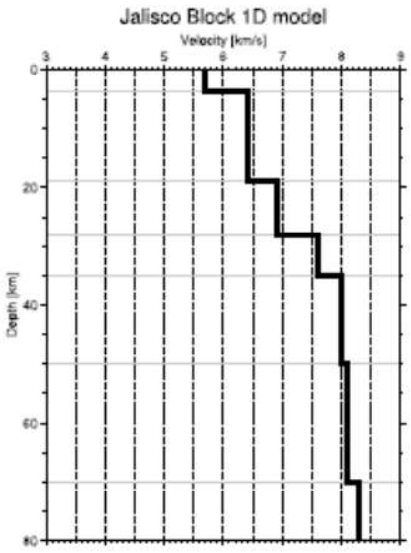

Figure 04

Figure 4. P-wave velocity model for Jalisco Block region (Núñez-Cornú *et al*., 2002).

The focal mechanism of the earthquakes was evaluated with the MEC93 code (Núñez-Cornú and Sánchez-Mora, 1999) using the outputs obtained from the Hypo71. The program MEC93 is based on a probabilistic model proposed by Brillinger *et al*. (1980). This method for focal mechanism estimation is also described by Udías *et al.* (1982), which uses a weighting parameter p, and a relation between readings and theoretical amplitude values, as a measure of the fit of a set of observations concerning the joint solution. A threshold value of p and a minimum of readings are selected to form a group with a joint solution. Also, a p_i value for each i event is defined as a function of the minimum and the maximum number of readings for all the events; this p_i is the threshold value to accept the event into the group.

Results and Discussions

The analysis of the first 115 earthquakes identified on helicorder records allowed us to obtain 54 events that could be read for enough stations; the remainder were too small and/or had station high signal-noise levels. Of the earthquakes processed, 39 achieved the standards mentioned before, but only 27 were in the area of interest (Table 1). All earthquakes relocated for the study period are shown in Fig. 2 and in Fig. 5a with error bars, while the depth profile projected along the EW line is shown in Fig. 5b. Figures 5a and 5b include the activity reported by Marín-Mesa *et al*. (2019). Our results show that there are two sub-parallel alignments with an approximate N-S direction at the western edge of the urban area (Fig. 2) lying in part of the GMZ and La Primavera Caldera, and from figure 5b it is possible to estimate a fault width (in-depth) of 10 -12 km in both. The western alignment crosses La Primavera Caldera, and the eastern one marks the "boundary" of the urban area and the contact between Atemajac and Tesistan volcanic structures (Fig. 2). The separation distance between the alignments is above 10 km (Fig. 5a).

The magnitude of the largest earthquake (M_L= 4.9) suggests a rupture area of 6 km^2 (4.0 x 1.5 km) with an approximate slip of 10 cm (Wyss, 1979; Hanks and Kanamori, 1979). Furthermore, we analyzed the distribution of the epicentral location error bars plotted in figure 5, where we can distinguish two groups. The first one is characterized by having errors in the epicentral location less than 5 km and corresponds to those epicenters outside La Primavera Caldera. The second group of epicenters is located within La Primavera Caldera with epicentral errors between 5 and 8 km and RMS values between 0.50 and 0.81. The difference in the residuals is due to the volcanic complex and heterogenic structure of La Primavera Caldera.

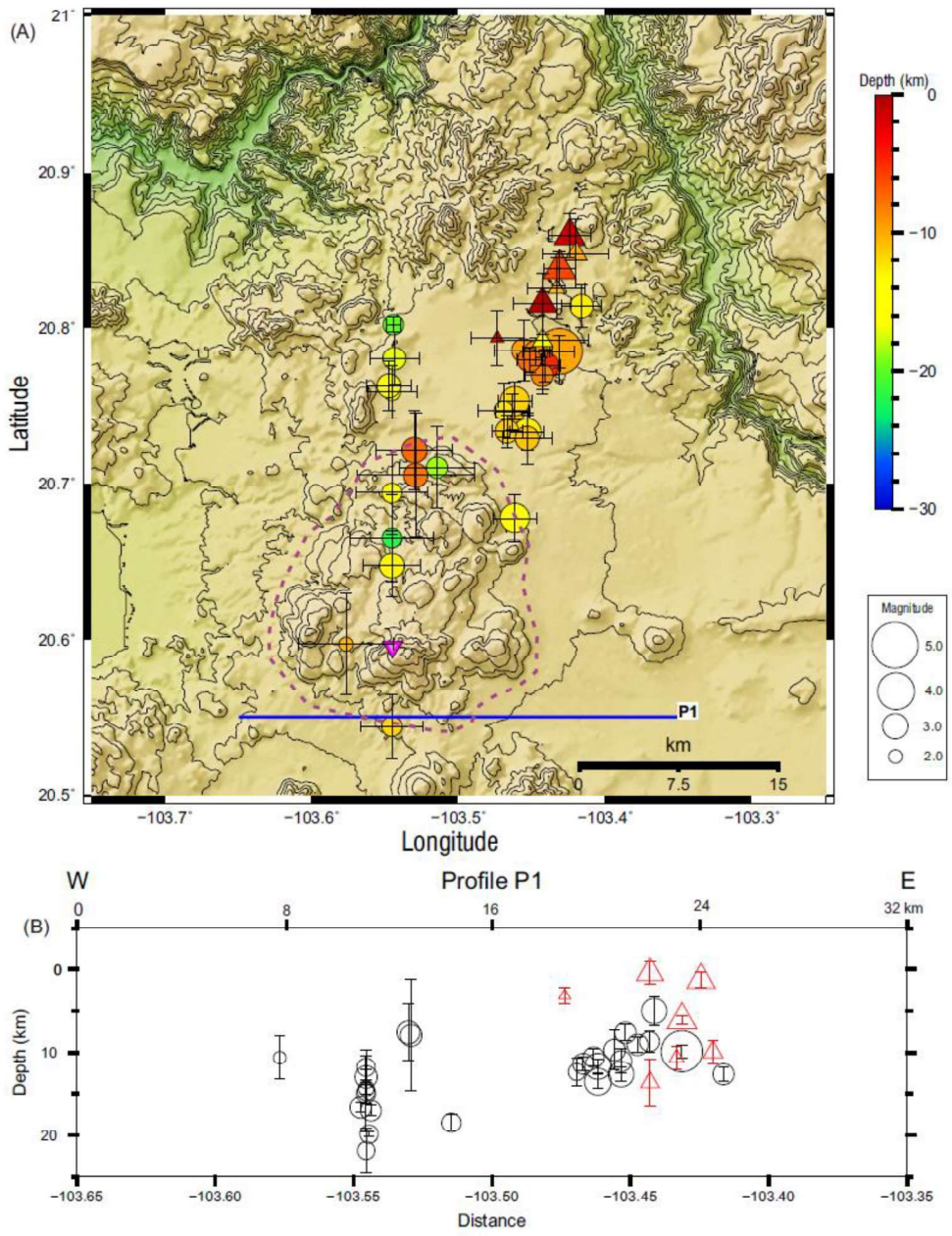

Figure 5. (**A**) Reported earthquakes (Triangles) for the period December 5 – 20 Marín-Mesa *et al.* (2019). Relocated earthquakes (circles) for period May 11-13, 2016 (Table 1) Error bars in km; Caldera La Primavera marked with dashed magenta line. Inverted triangle: Seismic station CPRJ. (**B**) Cross section along Profile P1 showing the hypocenters projected in a line E –W. Error bars in km.

To compare the differences in the source, we analyzed the waveforms recorded by MZCJ station for the largest earthquakes of the seismic swarm, which are shown in figure 6. This station is located near the city of Mazamitla (Fig. 3) on the east side of the Jalisco Block. The pathway to MZCJ station is very similar for all earthquakes, which are located at a distance between 95 and 112 km and with a 13° directional gap. It is possible to observe differences in the P and S waveforms, indicating different types of source processes and radiation patterns. At least five groups with waveform similarities can be found (Fig. 6). Earthquakes *w20*, *w16,* and *w14* are located in the western alignment, the rest in the eastern one. In the other groups, the epicenters are at a distance less than 5 km between them.

The focal mechanisms at the epicentral zone were evaluated from the take-off and azimuth angles generated by Hypo-71. Ten solutions, four individual mechanisms, and six composite mechanisms, or groups, (including 14 earthquakes) were obtained for a total of 18 earthquakes (Table 2), all with a P-polarity score (or success rate) of 80% or higher, and focal planes well-controlled (Fig. 7). From the total of the obtained mechanisms, 12 earthquakes show a normal fault mechanism, and 6 of them show an inverse fault mechanism. In both cases, the directions of the fault planes are congruent with the directions of the two seismic alignments observed from the epicentral locations that can also be observed at the figures 8a and 8b, where the data reported by Marín-Mesa *et al.* (2019) are included.

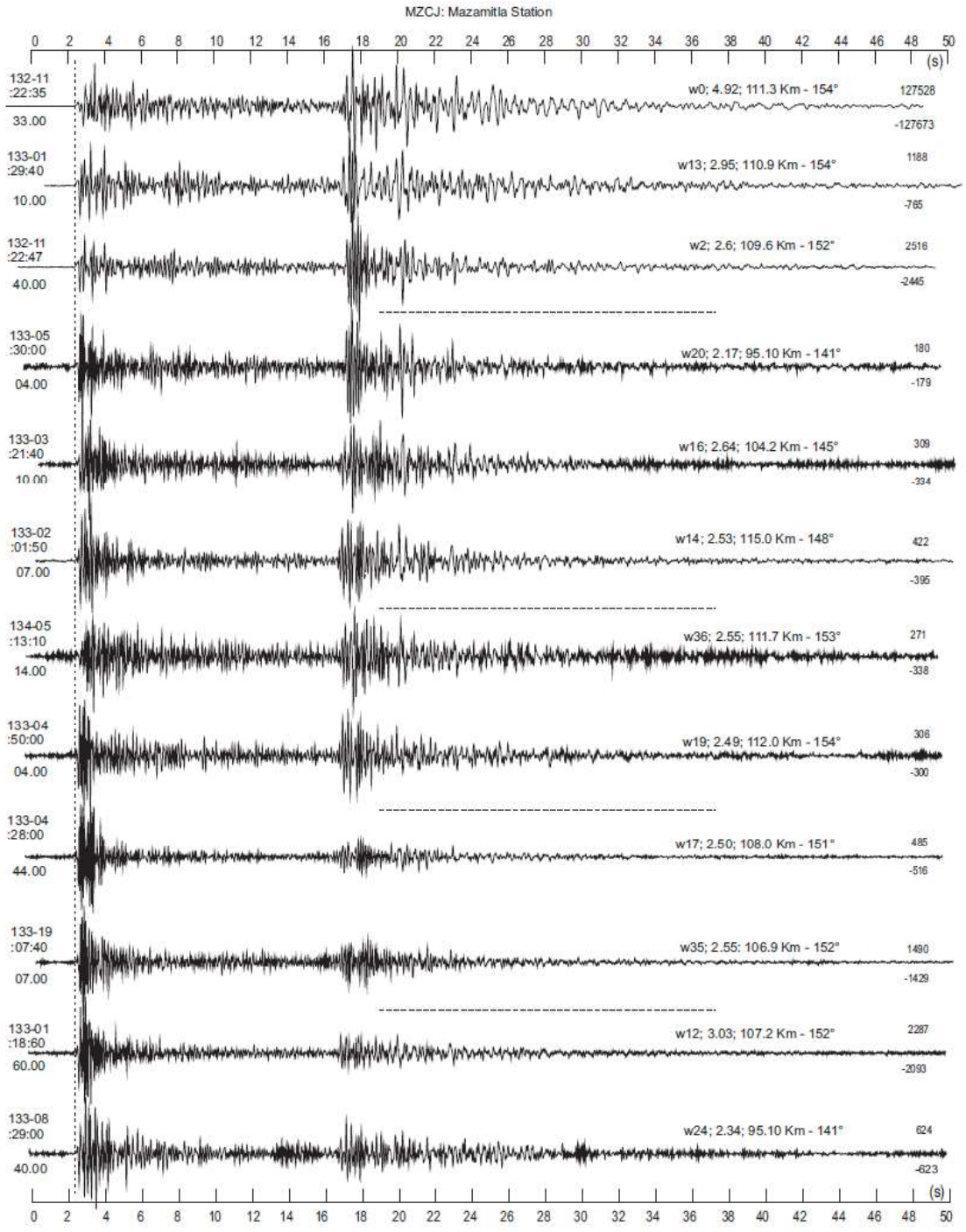

Figure 6

Figure 6. Waveforms (vertical component, not filtered) from the largest earthquakes of the May 11, 2016 earthquake swarm recorded at MCZJ Station (Fig. 3). For each trace, left side: above the trace T0 (origin time) of the earthquake, below the trace, the initial second of the trace. Above the trace: name of the earthquake, local magnitude, distance and azimuth from the epicenter. Right side: maximum and minimum amplitude in microvolts.

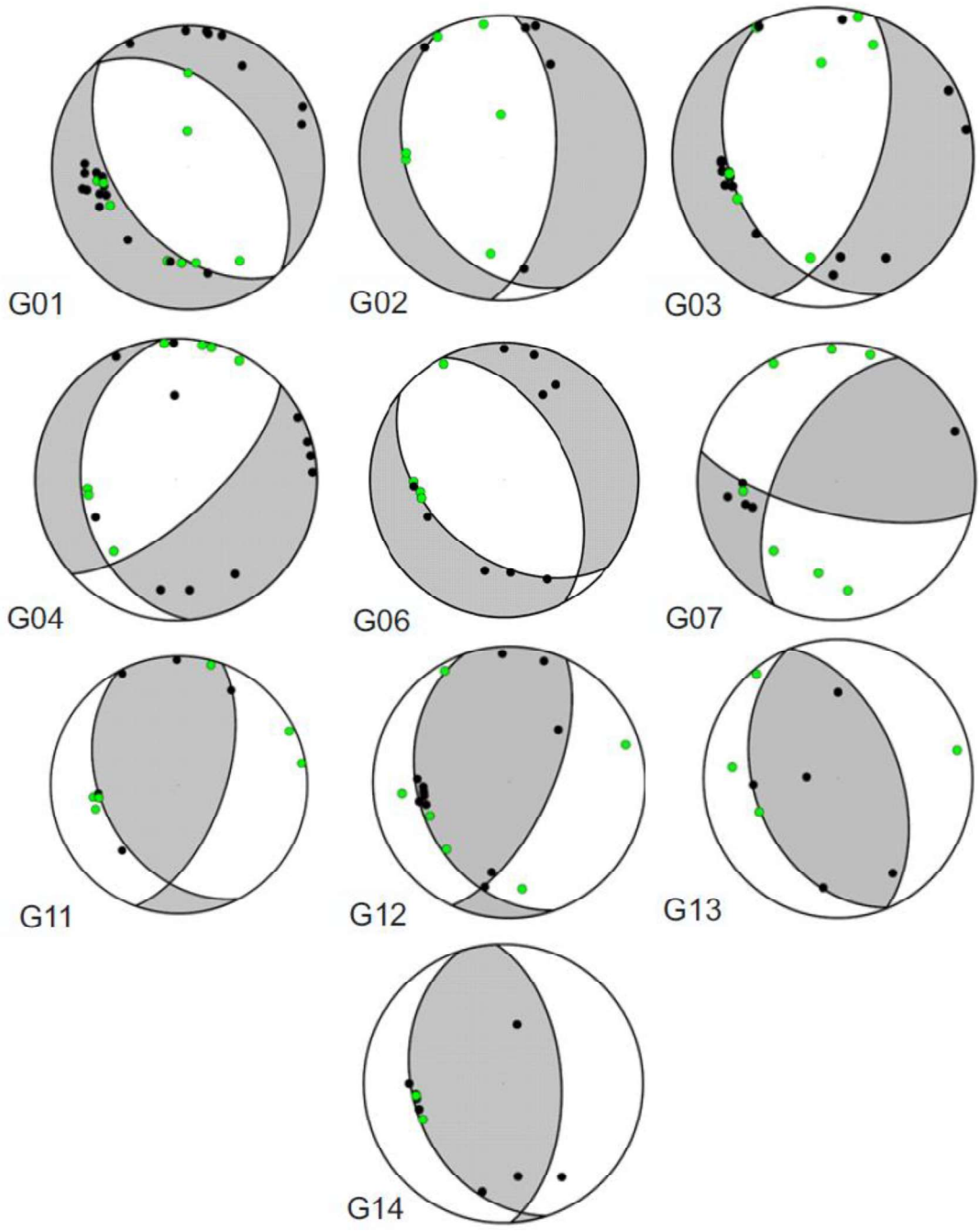

Figure 7. Focal Mechanism Solutions: four individual earthquakes (G07, G11, G12, G14) and five composite focal mechanisms (G01, G02, G03, G04, G06, G13) for 14 earthquakes. Solid black dots compressions, solid green dots dilatations (Table 2).

Group	Earthq.	Mag	Npol	%	Planes	Strike (°)	Dip (°)	Slip (°)	Axis	Plunge (°)	Azim (°)
01	w00	4.92	31	83	**Plane A**	140	47	-88	**P:**	2	90
	w21	2.06			**Plane B**	317	43	-88	**T:**	88	229
	w32	2.16									
02	w01	2.5	11	100	**Plane A**	155	34	-65	**P:**	19	311
	w16	2.64			**Plane B**	5	60	-74	**T:**	77	83
03	w06	1.38	27	85	**Plane A**	157	38	-53	**P:**	25	335
	w08	2.57			**Plane B**	20	60	-65	**T:**	78	92
	w19										
04	w13	2.95	18	83	**Plane A**	175	33	-42	**P:**	32	353
	w14	2.53			**Plane B**	48	69	-64	**T:**	70	119
06	w31	2.03	13	100	**Plane A**	129	41	-77	**P:**	11	344
	w26	2.51			**Plane B**	329	50	-75	**T:**	85	284
07	w35	2.55	12	92	**Plane A**	207	56	24	**P:**	80	158
					Plane B	103	71	37	**T:**	51	60
11	w24	2.34	11	82	**Plane A**	157	35	42	**P:**	72	101
					Plane B	30	68	63	**T:**	32	339
12	w07	3.16	18	83	**Plane A**	161	33	51	**P:**	73	98
					Plane B	25	65	68	**T:**	27	331
13	w15	2.43	9	100	**Plane A**	158	38	80	**P:**	82	61
	w29	1.5			**Plane B**	326	53	82	**T:**	10	202
14	w10	2.27	10	80	**Plane A**	162	35	78	**P:**	84	63
					Plane B	327	56	81	**T:**	6	201

379 Table 2. Parameters of the focal mechanism showed in Figure 8. *NPol*: Number of polarities readings.
380 %: score (or success rate) for *P* polarities.
381

382 The May 2016 seismic sequence began within the eastern alignment with the largest
383 earthquake, south of the swarm reported by Marín-Mesa *et al.* (2019), and the fourth locatable

earthquake occurred 15 min later within the western alignment (Figs. 8a and 8b). After that, both features were simultaneously active, but no hypocentral migration pattern was observed (Fig. 8b); the eastern alignment agrees with the alignment reported by Marín-Mesa *et al.* (2019). The main event is included in composite focal mechanism Group 01, showing a normal fault focal mechanism and suggesting an NNW – SSE fault with a P (090, 02) and T (229, 88) axis. The western alignment can be observed crossing La Primavera Caldera with NS direction (Fig. 8). Of the waveforms shown in figure 6, the earthquakes *w0*, *w13*, *w16*, *w14*, and *w19* have a normal fault mechanism; meanwhile, the earthquakes *w35* and *w24* have an inverse fault mechanism, with apparent differences in the waveforms.

The focal mechanisms within and adjacent to the study area have been obtained by recent seismicity and by ancient faults. Singh *et al.* (2017), using data from SSN, which had its closest station beyond 100 km from the epicenter, studied this earthquake and suggested that most of the events during the entire sequence were tightly clustered, probably within a volume of 1 to 2 km radius; this does not agree with our results. They also obtained normal fault mechanisms oriented NNE-SSW (azimuth of 021°) with tension axis at 110°. Yamamoto *et al.* (2018) also studied this earthquake using data from the SSN and other station; they suggested a strike-slip fault mechanism solution oriented SSE - NNW (azimuth of 158º) with a P (021°, 29°) and T (289°, 04°) axis. However, we obtain a normal fault mechanism with P (090°, 02°) and T (229°, 88°). Differences in these results may be due to the different models of velocities and datasets (azimuth coverage, distance to the epicenter, and the number of stations) were used in each case.

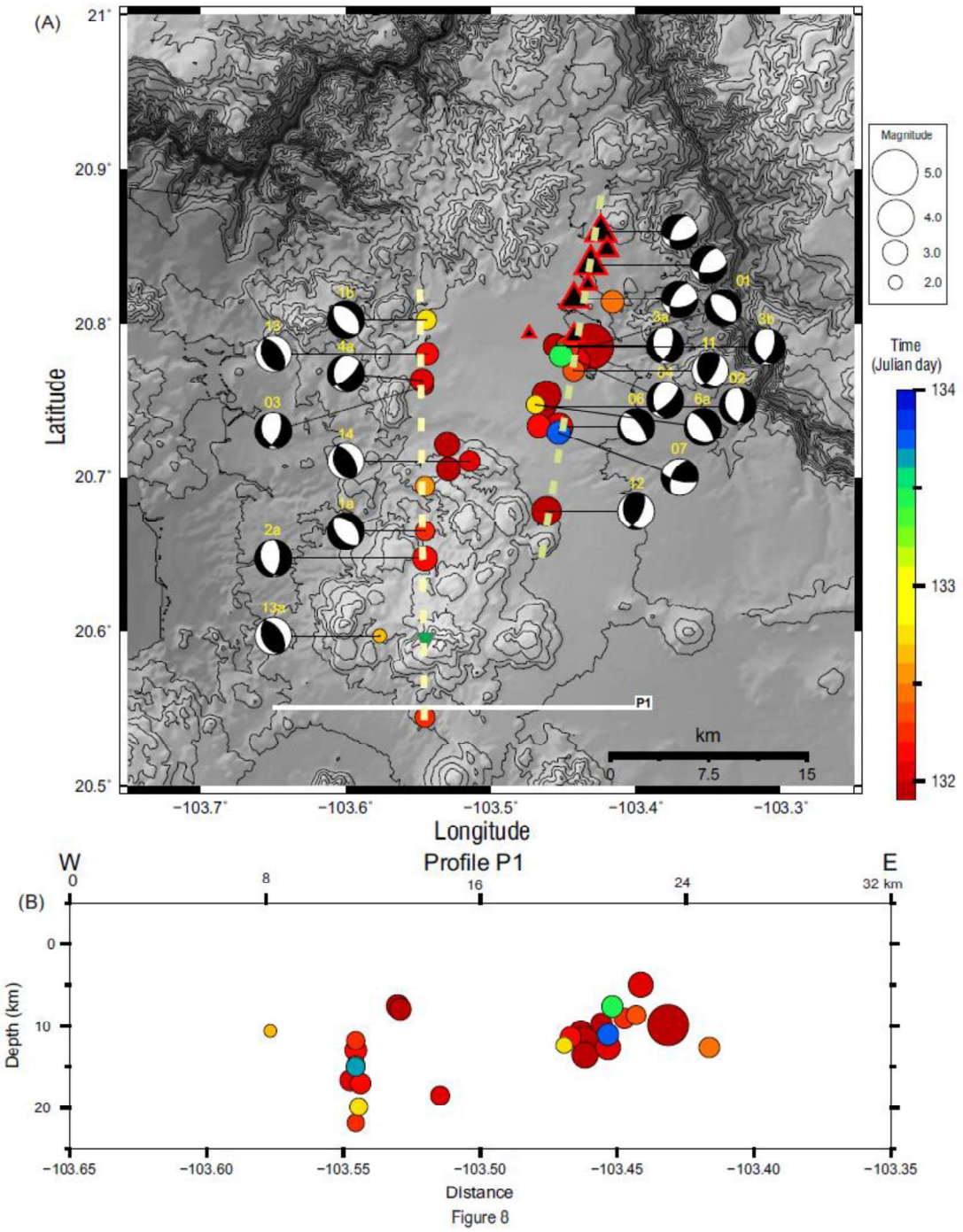

Figure 8. Time sequence: (**A**) Map of the epicenters with focal mechanism. (**B**) Cross section along Profile P1.

Most of the RESAJ stations are less than 200 km from the epicenter; meanwhile, most of the SSN stations have epicentral distances farther than 200 km. Our focal mechanism solution and the obtained by Singh *et al*. (2017) are a bit similar, and the polarity data of their focal mechanism are congruent with our results. The σ_3 orientations from ESE-WNW to ENE-WSW were also obtained from the preferred orientation the geological structures measured near the study area (Ferrari and Rosas-Elguera, 1999; Duque-Trujillo *et al.,* 2014). The N-S trend of the proposed Zapopan Graben follows the same trend as the Basin and Range structures defined in central Mexico (Nieto-Samaniego *et al.*, 1999; Aranda-Gómez *et al.*, 2000). So, this graben is apparently formed on reactivated structures (Moore *et al*., 1994; Frey *et al.*, 2007). On the other hand, the reverse focal mechanisms could be related to wrenching faults due to the right lateral movement component along the faults that define the Tepic-Zacoalco rift (Nieto *et al.*, 1985; Rodríguez-Castañeda and Rodríguez-Torres, 1992).

Conclusions

The hypocenters of the December 2015 and May 2016 seismic sequences show two apparent NS alignments west of the GMZ, and these structures have the same direction of the CR. The epicenters suggest the existence of two active quasi-parallel structures or faults separated about 10 km. The fault strikes obtained from the focal mechanisms coincide with the direction of the alignments. Using the waveforms recorded at MZCJ station, it is also possible to conclude that different types of sources took place during the seismic sequence.

444 Furthermore, the solutions of most of these mechanisms correspond to a normal fault,
445 suggesting the existence of a graben, which we propose as Zapopan Graben. The western
446 fault crosses La Primavera Caldera. In the central part of the eastern fault, the structural
447 features are not visible on the ground owing to the urban development. The proposed length
448 of the eastern fault is approximately 21 km (including the December 2015 segment), and the
449 western fault is 28 km. From the hypocentral depths of the seismic sequence, it is possible to
450 assume a fault width of approximately 10 km, so the maximum earthquakes that could be
451 generated by these faults would be approximate of magnitudes 6.3 and 6.5, respectively.

452 Moreover, these faults are shallow so that these earthquakes could cause significant damage
453 as the 1847b Ocotlán earthquake (Suter, 2018) and the historical damage reported. More
454 geophysical and geological studies are needed to confirm the existence of these tectonic
455 structures. However, the macroseismic reports from these seismic sequences are not
456 comparable to the historical reports about seismic sequence previously mentioned; only the
457 mainshocks were felt by most of population, and not relevant damages were reported. Recent
458 microseismicity studies at La Primavera Caldera (Quinteros-Cartaya *et al*., 2020) reports
459 microearthquake activity (M_L <3.0) inside the proposed Zapopan Graben. This proposed
460 graben could be the source of the historical seismic sequences that occurred at GMZ.

461 The GMZ is the second-largest urban area of Mexico, and unlike Mexico City, where there
462 are historical reports of local seismicity up to at least magnitude 6.0 representing a significant
463 seismic hazard that must be studied and evaluated in great detail. Particularly noteworthy are
464 these studies for the development of the Cerritos Colorados Geothermal Field in La
465 Primavera Caldera. As a result of this study, the research group CA-UDG-276 (SisVOc) is

carrying out a joint project with the Zapopan Civil Defense Authorities to install a seismic network in the municipality of Zapopan.

DATA AND RESOURCES

All seismic data collected by RESAJ are in a database at CA-UDG-276 SisVOc Research Group. The data may be available for use in collaborative research projects between SisVOc and other interested institutions by specific agreements. For information, contact pacornu77@gmail.com.

Funding

This Research is funded by Projects: Centro Mexicano de Innovación en Energía – Geotérmica (CeMIE-Geo). P24. Proyecto Secretaría de Energía - Consejo Nacional de Ciencia y Tecnología (SENER-CONACyT) 201301-207032; Consejo Nacional de Ciencia y Tecnología – Fondos Mixtos Jalisco (CONACyT-FOMIXJal) 2008-96567 (2009); CONACyT–FOMIXJal 2008-96539 (2009); CONACyT-FOMIXJal 2010-149245 (2010) and Universidad de Guadalajara internal Projects; Walter M. Rengifo was funded by a Master scholarship from CONACyT, CVU 596343, Reg. 572768.

Acknowledgments

The authors are grateful to anonymous reviewers for a thorough review and constructive suggestions that improve the quality of this article, also would like to thank Quiriat J. Gutiérrez-Peña for his assistance during the data selection and processing stages of this work.

References

Allan, J.F. (1986). Geology of the northern Colima and Zacoalco grabens, southwest Mexico: Late Cenozoic rifting in the Mexican Volcanic Belt. Geol. Soc. Am. Bull. 97, 473-485.

492 Allan, J.F., Nelson, J., Luhr, J., Carmichael, J., Wopat, M. and Wallace, P. (1991). Pliocene-
493 Recent rifting in SW México and associated volcanism: An exotic terrane in the
494 making. Am. Assoc. Petrol. Geol. Mem. 47, 425-445.
495 Aranda-Gómez, J.J., Henry, C.D. and Luhr, J.F. (2000). Evolución tectonomagmática post-
496 paleocénica de la Sierra Madre Occidental y de la porción meridional de la provincia
497 tectónica de Cuencas y Sierras, México. Bol. Soc. Geol. Mex. LIII, 59-71
498 Arreola-Ochoa, M.C. (2015) Del pulpito a las estrellas, Don José María Arreola Mendoza
499 sacerdote, astrónomo y vulcanólogo. Secretaría de Cultura del Gobierno de Jalisco.
500 171 pp.
501 Bandy, W.L., Mortera-Gutiérez, C., Urrutia-Fucugauchi, J. and Hide, T.W. (1995). The
502 subducted Rivera-Cocos plate boundary: Where is it, and what is its relationship to
503 the Colima rift? Geophys. Res. Lett. 22, 3075-3078.
504 Bourgois, J. and Michaud F. (1991). Active fragmentation of the North America plate at the
505 Mexican Triple Junction area off Manzanillo. Geo-Marine Lett. 11, 59-65.
506 Brillinger, D., Udías, A. and Bolt, B. (1980). A probability model for regional focal
507 mechanism solutions. Bull. Seismol. Soc. Am. 70, 1479–1485.
508 DeMets, C. and Stein, S. (1990). Present-day kinematics of the Rivera Plate and implications
509 for tectonics of Southwestern Mexico. J. Geophys. Res. 95, 21931-21948.
510 Dirección General de Estadística (1910). Tercer Censo de Población de los Estados Unidos
511 Mexicanos.
512 Duque-Trujillo, J., Ferrari, L., Norini, G. and López-Martínez, M. (2014). Miocene faulting
513 in the southwestern Sierra Madre Occidental, Nayarit, Mexico: kinematics and
514 segmentation during the initial rifting of the southern Gulf of California. Rev. Mex.
515 Cien. Geol. 31, 283-302.

516 Ferrari, L. and Rosas-Elguera, J. (1999). Late Miocene to Quaternary extension at the
517 northern boundary of the Jalisco Block, western Mexico: The Tepic-Zacoalco rift
518 revisited. In H. Delgado-Granados, G. Aguirre-Díaz and J.M. Stock, J.M., eds.,
519 Cenozoic Tectonics and Volcanism of Mexico. Geol. Soc. Am. Special Paper 334, 1-
520 23.
521 Ferrari, L., Pasquarè, G., Venegas, S., Castillo, D. and Romero, F. (1994). Regional tectonics
522 of western Mexico and its implications for the northern boundary of the Jalisco Block.
523 Geof. Intern. 33, 139-151.
524 Frey, H.M., Lange, R.A., Hall, C.M., Delgado-Granados, H. and Carmichael, I.S. (2007). A
525 Pliocene ignimbrite flare-up along the Tepic-Zacoalco rift: Evidence for the initial
526 stages of rifting between the Jalisco block (Mexico) and North America. Geol. Soc.
527 Am. Bull. 119, 49-64; doi: 10.1130/B25950.1
528 Hanks, T., and Kanamori, H. (1997). A moment magnitude scale: J. Geoph. Res. 84, 2348-
529 2350.
530 Haskov, J. and Ottemoller, L. (1999). Seisan earthquake analysis software. Seism. Res. Lett.
531 70, 532-534.
532 Kostoglodov, V. and Bandy, W. (1995). Seismotectonic constraints on the convergence rate
533 between the Rivera and North America plates. J. Geophys. Res. 100, 17977-17989.
534 Lay, T. and T. Wallace. (1995). Modern Global Seismology. Academic Press, 523 pp.
535 Lee, W.H.K. and Lahr. J.A. (1972). HYPO71: A Computer Program for Determining
536 Hypocenter, Magnitude and First Motion Pattern of Local Earthquakes. U.S.
537 Geological Survey Open-File Report 100 pp.

538 Lindquist, K.G., Newman, R.L., and Vernon, F.L. (2007). The antelope interface to PHP and
539 applications: Web-based real-time monitoring. Seismol. Res. Lett. 78 (6) 663-670,
540 doi:10.17885/gssrl.78.6.663.
541 Luhr, J., S. Nelson, S., Allan J. and Carmichael, I. (1985). Active rifting in southwestern
542 Mexico: Manifestations of an incipient eastward spreading-ridge jump. Geology 13,
543 54-57.
544 Maciel-Flores, R. and Rosas-Elguera, J. (1992). Modelo geológico y evaluación del campo
545 geotérmico La Primavera, Jal., México. Geof. Intern. 31, 359-370.
546 Marín-Mesa, T., Núñez-Cornú, F.J. and Suárez-Plascencia, C. (2019). Analysis of the
547 seismicity in the Jalisco Block from June to December 2015. Seism. Res. Lett.
548 Vol.90-5:1767-1778. (doi: 10.1785/0220190107).
549 Martínez-Gracida, M. (1886). Terremotos en Oaxaca. Unpublished manuscript. Casa de la
550 Cultura, Oaxaca, 70 pp.
551 Matute, J.I. (1875). Temblores observados en Guadalajara y otros puntos en el mes de junio
552 de 1875, en Informe y colección de Artículos relativos a los fenómenos geológicos
553 verificados en Jalisco en el presente año y en épocas anteriores, Tomo I. Tipografía
554 de S. Banda, c/ de la Maestranza 4. Guadalajara. 80 pp.
555 Minster, J. and Jordan, H. (1978). Present-day plate motion. J. Geophys. Res. 83, 5331-5354.
556 Moore, G., Marone, C., Carmichael, I.S.E. and Renne, P. (1994). Basaltic volcanism and
557 extension near the intersection of the Sierra Madre volcanic province and the Mexican
558 Volcanic Belt. Geol. Soc. Am. Bull. 106, 383-394.
559 Nieto-Obregón, J., Delgado-Argote, L.A. and Damon, P.E. (1985). Geochronologic,
560 petrologic and structural data related to large morphological features between the
561 Sierra Madre Occidental and the Mexican Volcanic Belt. Geof. Intern. 24, 623-663.

562 Nieto-Samaniego, A.A., Ferrari, L., Alaniz-Álvarez, S.A. and Rosas-Elguera, J. (1999).
563 Variation of Cenozoic extensión and volcanism across the southern Sierra Madre
564 Occidental volcanic province, Mexico. Geol. Soc. Am. Bull. 111, 347-363.
565 Núñez-Cornú, F. and Sánchez-Mora, C. (1999). Stress field estimations for Colima Volcano,
566 México, based on seismic data. Bull. Volcanol. 60, 568–580
567 Núñez-Cornú, F., Rutz, M., Nava., F.A., Reyes-Dávila, G. and Suárez-Plascencia, C. (2002).
568 Characteristics of the Seismicity in the Coast and North of Jalisco Block, Mexico.
569 Phys. Earth Planet. Int. 132, 141-155.
570 Núñez- Cornú, F.J. (2011). Peligro Sísmico en el Bloque de Jalisco. Fís. Tierra. 29, 199-229.
571 doi: dx.doi.org/10.5209/rev_FITE.2011v23.36919.
572 Núñez-Cornú, F.J., Sandoval, J.M., Gómez, A., Alarcón, E., Suarez-Plascencia, C., Núñez,
573 D., Trejo-Gómez, E., Sánchez-Mariscal, O. and Candelas-Ortiz., J.G. (2018). The
574 Jalisco Seismic Accelerometric Telemetric Network (RESAJ). Seismol. Res. Lett. 89
575 (2A), 363-372. doi: 10.1785/0220170157.
576 Ordoñez, E. (1912). The Recent Guadalajara Earthquakes. Bull. Soc. Seismol. Am. 2 (2), 134
577 -137.
578 Orozco y Berra, J. (1887). Efemérides Sísmicas Mexicanas. Memorias de la Soc. Cientif.
579 “Antonio Alzate”, Tomos I and II.
580 Quinteros-Cartaya, C., Solorio-Magaña, G., Núñez-Cornú, F.J., Núñez, D. and Sandoval,
581 J.M. (2020). Análisis de la Actividad Sísmica ocurrida durante el 2017, en la Zona
582 Metropolitana de Guadalajara y sus Alrededores. Reunión Anual 2019 de la Unión
583 Geofísica Mexicana, Puerto Vallarta Jal., Geos 39 (2), 214.
584 Righter, K. and Carmichael, I.S. (1992). Hawaiites, and related lavas in the Atenguillo
585 graben, western Mexican Volcanic Belt. Geol. Soc. Am. Bull. 104, 1592-1607.

586 Rodríguez-Castañeda, J.L. and Rodríguez-Torres, R. (1992). Geología estructural y
587 estratigrafía del área entre Guadalajara y Tepic, estados de Jalisco y Nayarit, México.
588 Universidad Nacional Autónoma de México, Inst. Geol., Revista, 10, 99-110.
589 Rosas-Elguera, J., Ferrari, L., Garduño-Monroy, V.H. and Urrutia-Fucugauchi, J. (1996).
590 Continental boundaries of the Jalisco block and their influence in the Pliocene-
591 Quaternary kinematics of western Mexico. Geology, 24, 921-924.
592 Rossotti, A., Ferrari, L., López-Martínez, M. and Rosas-Elguera, J. (2002). Geology of the
593 boundary between the Sierra Madre Occidental and the Trans-Mexican Volcanic Belt
594 in the Guadalajara region, western Mexico. Rev. Mex. Cien. Geol. 19, 1-15.
595 Selvans, M.M., Stock, J.M., DeMets, C. and Sánchez, O. (2011). Constraints on Jalisco block
596 motion and tectonics of the Guadalajara triple junction from 1998-2001 campaign
597 GPS data. Pure Appl. Geophys. 168, 1435-1447.
598 Sing, S.K., Rodríguez, M. and Espíndola, J.M. (1984). A Catalog of Shallow Earthquakes of
599 Mexico from 1900 to 1981. Bull. Seimol. Soc. Am. 74 (1), 267-279.
600 Singh, S.K, Arroyo, D., Pérez-Campos, X., Iglesias, A., Espíndola, V.H. and Ramírez, L.
601 (2017). Guadalajara, Mexico, Earthquake Sequence of December 2015 and May
602 2016: Source, Q, and Ground Motion. Geofis. Intern. 56 (2), 173-186.
603 Suter, M. (2015). The A.D. 1567 Mw 7.2 Ameca, Jalisco, Earthquake (Western Trans-
604 Mexican Volcanic Belt): Surface Rupture Parameters, Seismogeological Effects, and
605 Macroseismic Intensity from Historical Sources. Bull. Seismol. Soc. Am. 105 (2A),
606 646-656. Doi: 10.1785/0120140163.
607 Suter, M. (2018). The 2 October 1847 Ml 5.7 Chapala Graben Triggered Earthquake (Trans-
608 Mexican Volcanic Belt, West Central Mexico: Macroseismic Observations and
609 Hazard Implications. Seismol. Res. Lett. 89 (1), 35-46. doi: 10.1785/0220170101.

610 Suter, M. (2019a). The 1563 MI 8 Puerto de la Navidad Subduction-Zone and 1567 Mw 7.2
611 Ameca Crustal Earthquakes (Western Mexico): New Insights from Sixteenth-Century
612 Sources. Seismol. Res. Lett. 90 (1), 366-375 doi: 10.1785/0220180304.
613 Suter, M. (2019b). Macrosismic Study of the Devastating 22-23 October 1749 Earthquake
614 Doublet in the Northern Coima Graben (Trans-Mexican Volcanic Belt, Western
615 Mexico). Seismol. Res. Lett. 90 (6). 2304-2317. doi: 10.1785/0220190162.
616 Suter, M. (2020a). The 6 November 1774 Mi 6 Bolañoz Graben Earthquake (Southern Basin
617 and Range Province, West –Central Mexico): Macrosismic Observations and
618 Neotectonic Implications. Seismol. Res. Lett. XX (1), 366-37546. doi:
619 10.1785/0220200016.
620 Suter, M. (2020b). Comment on "Active Crustal Deformation in the Trans-Mexican Volcanic
621 Belt as Evidenced by Historical Earthquakes during the Last 450 years" by Suárez et
622 al. (2019). Tectonics, 39 (in press). doi: 10.1029/2019TC006016.
623 Udías, A., Buforn, E., Brillinger, D. and Bolt, B. (1982) Joint statistical determination of
624 fault-plane parameters. Phys. Earth Planet Int. 30, 178–184.
625 Waitz and Urbina (1919). Reporte de los sismos ocurridos en la Ciudad de Guadalajara en
626 1912. Instituto Geológico de México, Secretaria de Industria, Comercio y Trabajo. p.
627 129.
628 Wessel, P. and Smith, W.H.F. (1998). New, improved version of generic mapping tools
629 released. EOS Trans. AGU 79, 579.
630 Wyss, M. (1979). Estimating maximum expectable magnitude of earthquakes from fault
631 dimensions. Geology 7, 336-340.
632 Yamamoto, J., Espíndola J.M., Zamora-Camacho A. and Castellanos G. (2018). The origin
633 of the recent (2012 - 2016) seismic activity in the Guadalajara, Jalisco, Mexico, area:

634 A block boundary interaction? PLoS ONE 13 (8): e0200991. https://doi.org/10.1371/
635 journal.pone.0200991

636

637